Inorg. Chem. **2006**, *45*, 2413–2423

2,4,6-Tris(2-pyridyl)-1,3,5-triazine (tptz)-Derived $[Ru^{II}(tptz)(acac)(CH_3CN)]^+$ and Mixed-Valent $[(acac)_2Ru^{III}\{(\mu\text{-tptz-}H^+)^-\}Ru^{II}(acac)(CH_3CN)]^{+}$†

Sandeep Ghumaan,‡ Sanjib Kar,‡ Shaikh M. Mobin,‡ B. Harish,‡ Vedavati G. Puranik,§ and Goutam Kumar Lahiri*,‡

Department of Chemistry, Indian Institute of Technology—Bombay, Powai, Mumbai 400076, India, and Center for Materials Characterization, National Chemical Laboratory, Pune, Maharashtra 411008, India

Received August 22, 2005

Mononuclear $[Ru^{II}(tptz)(acac)(CH_3CN)]ClO_4$ ([**1**]ClO_4) and mixed-valent dinuclear $[(acac)_2Ru^{III}\{(\mu\text{-tptz-}H^+)^-\}Ru^{II}(acac)(CH_3CN)]ClO_4$ ([**5**]ClO_4; acac = acetylacetonate) complexes have been synthesized via the reactions of $Ru^{II}(acac)_2(CH_3CN)_2$ and 2,4,6-tris(2-pyridyl)-1,3,5-triazine (tptz), in 1:1 and 2:1 molar ratios, respectively. In [**1**]ClO_4, tptz binds with the Ru^{II} ion in a tridentate N,N,N mode (motif **A**), whereas in [**5**]ClO_4, tptz bridges the metal ions unsymmetrically via the tridentate neutral N,N,N mode with the Ru^{II} center and cyclometalated N,C^- state with the Ru^{III} site (motif **F**). The activation of the coordinated nitrile function in [**1**]ClO_4 and [**5**]ClO_4 in the presence of ethanol and alkylamine leads to the formation of iminoester ([**2**]ClO_4 and [**7**]ClO_4) and amidine ([**4**]ClO_4) derivatives, respectively. Crystal structure analysis of [**2**]ClO_4 reveals the formation of a beautiful eight-membered water cluster having a chair conformation. The cluster is H-bonded to the pendant pyridyl ring N of tptz and also with the O atom of the perchlorate ion, which, in turn, makes short (C–H- - - -O) contacts with the neighboring molecule, leading to a H-bonding network. The redox potentials corresponding to the Ru^{II} state in both the mononuclear $\{[(acac)(tptz)Ru^{II}\text{–}N{\equiv}C\text{–}CH_3]ClO_4$ ([**1**]ClO_4) ≫ $[(acac)(tptz)Ru^{II}\text{–}NH{=}C(CH_3)\text{–}OC_2H_5]ClO_4$ ([**2**]ClO_4) > $[(acac)(tptz)Ru^{II}\text{–}NH_2\text{–}C_6H_4(CH_3)]ClO_4$ ([**3**]ClO_4) > $[(acac)(tptz)Ru^{II}\text{–}NH{=}C(CH_3)\text{–}NHC_2H_5]ClO_4$ ([**4**]ClO_4)$\}$ and dinuclear $\{[(acac)_2Ru^{III}\{(\mu\text{-tptz-}H^+)^-\}Ru^{II}(acac)(N{\equiv}C\text{–}CH_3)]ClO_4$ ([**6**]ClO_4), $[(acac)_2Ru^{III}\{(\mu\text{-tptz-}H^+)^-\}Ru^{II}(acac)(NH{=}C(CH_3)\text{–}OC_2H_5)]ClO_4$ ([**7**]ClO_4), and $[(acac)_2Ru^{III}\{(\mu\text{-tptz-}H^+)^-\}Ru^{II}(acac)(NC_4H_4N)]ClO_4$ ([**8**]ClO_4)$\}$ complexes vary systematically depending on the electronic nature of the coordinated sixth ligands. However, potentials involving the Ru^{III} center in the dinuclear complexes remain more or less invariant. The mixed-valent $Ru^{II}Ru^{III}$ species ([**5**]ClO_4–[**8**]ClO_4) exhibits high comproportionation constant (K_c) values of 1.1×10^{12}–2×10^9, with substantial contribution from the donor center asymmetry at the two metal sites. Complexes display Ru^{II}- and Ru^{III}-based metal-to-ligand and ligand-to-metal charge-transfer transitions, respectively, in the visible region and ligand-based transitions in the UV region. In spite of reasonably high K_c values for [**5**]ClO_4–[**8**]ClO_4, the expected intervalence charge-transfer transitions did not resolve in the typical near-IR region up to 2000 nm. The paramagnetic $Ru^{II}Ru^{III}$ species ([**5**]ClO_4–[**8**]ClO_4) displays rhombic electron paramagnetic resonance (EPR) spectra at 77 K ($\langle g\rangle \sim 2.15$ and $\Delta g \sim 0.5$), typical of a low-spin Ru^{III} ion in a distorted octahedral environment. The one-electron-reduced tptz complexes $[Ru^{II}(tptz^{\bullet-})(acac)(CH_3CN)]$ (**1**) and $[(acac)_2Ru^{III}\{(\mu\text{-tptz-}H^+)^{\bullet 2-}\}Ru^{II}(acac)(CH_3CN)]$ (**5**), however, show a free-radical-type EPR signal near $g = 2.0$ with partial metal contribution.

Introduction

2,4,6-Tris(2-pyridyl)-1,3,5-triazine (tptz) has long been used as an analytical reagent[1] and more recently for developing metal complexes with diverse perspectives.[2] However, Ru chemistry of tptz has been confined to a limited number of mononuclear and dinuclear complexes.[3] In principle, tptz can bind to the metal ions in a number of ways and the motifs **A**, **B** and **C**, **D** (Chart 1) have indeed been reported for mononuclear[3a–o] and dinuclear[3p–r] Ru complexes, respectively. The trinucleating mode of tptz (motif **E**) though has been mentioned in one report.[4]

Moreover, Ru-ion-mediated intramolecular hydroxylation of the coordinated tptz unit[3c] and DNA binding[3b,n] properties of Ru−tptz complexes have also been explored.

† Dedicated to Professor Wolfgang Kaim, Institut fuer Anorganische Chemie, Universitaet Stuttgart, Pfaffenwaldring 55, D-70550 Stuttgart, Germany, on the occasion of his 55th birthday.

* To whom correspondence should be addressed. E-mail: lahiri@chem.iitb.ac.in.

‡ Indian Institute of Technology—Bombay.

§ National Chemical Laboratory.

10.1021/ic0514288 CCC: $33.50
Published on Web 02/16/2006

Chart 1

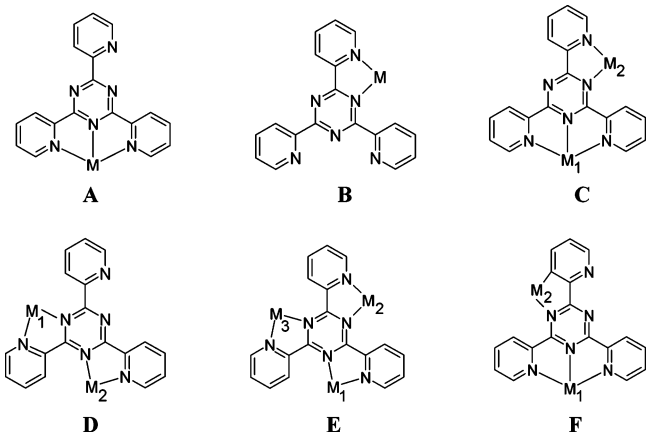

In the reported systems, the ancillary ligands associated with the Ru−tptz unit were mostly π acceptor in nature, either 2,2′:6′,2″-terpyridine, 2,2′-bipyridine (bpy), 1,10-phenanthroline, CO, or $PPh_3/AsPh_3$, etc.[3] Therefore, the present work deals with the perspective of further exploration of the metalation aspects of tptz with the Ru precursor unit $\{Ru(acac)_2\}$, encompassing an electronically rich acetylacetonate ($acac^-$) group. The choice of "$acac^-$" as the ancillary ligand for the present study originates from our recent observations that the presence of the "$acac^-$" unit with the Ru ion instead of π-acidic bpy-like ligands makes significant differences toward the overall energetics and subsequent chemical behaviors of the complexes.[5] Thus, the interaction of $Ru(acac)_2(CH_3CN)_2$ with tptz has led to the formations of hitherto unprecedented mixed-valent $Ru^{II}Ru^{III}$ species, [**5**]ClO_4 having motif **F** and the corresponding mononuclear Ru^{II} complex [**1**]ClO_4 (motif **A**). Further, the relatively electrophilic nitrile function in both the mononuclear [**1**]ClO_4 and dinuclear [**5**]ClO_4 complexes has undergone direct transformations to the coordinated iminoester ([**2**]ClO_4 and [**7**]ClO_4) and amidine ([**4**]ClO_4) derivatives in the presence of protic nucleophiles, alcohol, and alkylamine, respectively.

In this paper, the detailed synthetic account of the complexes [**1**]ClO_4−[**8**]ClO_4 (Scheme 1), crystal structures of selective derivatives, spectroelectrochemical properties, and the substitution/activation processes of the coordinated nitrile function in [**1**]ClO_4 and [**5**]ClO_4 have been deliberated.

Results and Discussion

Synthesis. The mononuclear [**1**]ClO_4 (motif **A**) and dinuclear [**5**]ClO_4 (motif **F**) complexes were synthesized via the reactions of precursor complex $Ru(acac)_2(CH_3CN)_2$ with tptz in molar ratios of 1:1 and 2:1, respectively, in refluxing ethanol followed by chromatographic purifications using an alumina column (Scheme 1). The formation of [**1**]ClO_4 has been authenticated by its single-crystal X-ray structure (see later). The dinuclear complex [**5**]ClO_4 could also be synthesized in quantitative yield starting from the mononuclear derivative [**1**]ClO_4 in the presence of excess metal precursor $[Ru(acac)_2(CH_3CN)_2]$. All of our attempts to synthesize the trinuclear derivative (motif **E**) using 3:1 or higher molar ratios of the Ru precursor complex and tptz or from the preformed [**1**]ClO_4 as well as [**5**]ClO_4 failed altogether. The reaction always ended up yielding the dinuclear species, [**5**]ClO_4.

The effect of π-accepting tptz and electron-withdrawing CH_3CN ligands in the coordination sphere of [**1**]ClO_4 has been reflected in its reasonably high $Ru^{III}-Ru^{II}$ potential (~0.8 V vs SCE; see later). The mixed-valent $Ru^{II}Ru^{III}$ state in the dinuclear complex [**5**]ClO_4 (motif **F**) develops via the formation of a Ru−C^- bond from the pendant pyridine ring of tptz to the second metal ion in addition to its linkage with the two electronically rich $acac^-$ units. It may be noted that the Ru-ion-induced selective C−H bond activation of the pyridazyl ring and subsequent stabilization of the mixed-valent $Ru^{II}Ru^{III}$ state in $[Ru^{II}\{N(pyridyl), N(pyridazyl)O_4(acac^-)_2\}Ru^{III}\{N(pyridyl),C^-(pyridazyl)O_4(acac^-)_2\}]$ has been reported recently.[5e] Similarly, cyclometalation via the C−H bond activation of the pyridine ring of diimine-based ligands is also known.[6]

(1) (a) Janmohamed, M. J.; Ayres, G. H. *Anal. Chem.* **1972**, *44*, 2263. (b) Embry, W. A.; Ayres, G. H. *Anal. Chem.* **1968**, *40*, 1499. (c) Tsen, C. C. *Anal. Chem.* **1961**, *33*, 849. (d) Diehl, H.; Buchanan, E. B., Jr.; Smith, G. G. *Anal. Chem.* **1960**, *33*, 1117. (e) Collins, P. F.; Diehl, H. *Anal. Chim. Acta* **1960**, *22*, 125. (f) Collins, P. F.; Diehl, H.; Smith, G. F. *Anal. Chem.* **1959**, *31*, 1862.

(2) (a) Paul, P.; Tyagi, B.; Bilakhiya, A. K.; Bhadbhade, M. M.; Suresh, E.; Ramachandraiah, G. *Inorg. Chem.* **1998**, *37*, 5733. (b) Folgado, J.-V.; Henke, W.; Allmann, R.; Stratemeier, H.; Beltrán-Porter, D.; Rojo, T.; Reinen, D. *Inorg. Chem.* **1990**, *29*, 2035. (c) Geling, A.; Olsen, M. D.; Orell, K. G.; Osborne, A. G.; Sik, V. *J. Chem. Soc., Chem. Commun.* **1997**, 587. (d) Arif, A. M.; Hart, F. A.; Hursthouse, M. B.; Thornton-Pett, M.; Zhu, W. *J. Chem. Soc., Dalton Trans.* **1984**, 2449. (e) Sedney, D.; Kahjehnassiri, M.; Reiff, W. M. *Inorg. Chem.* **1981**, *20*, 3476. (f) Prasad, J.; Peterson. N. C. *Inorg. Chem.* **1971**, *10*, 88. (g) Fraser, F. H.; Epstein, P.; Macero, D. J. *Inorg. Chem.* **1972**, *11*, 2031. (h) Faus, J.; Julve, M.; Amigo, J. M.; Debaerdemaeker, T. *J. Chem. Soc., Dalton Trans.* **1989**, *9*, 1681. (i) Chen, X.; Femia, F. J.; Babich, J. W.; Zubieta, J. A. *Inorg. Chem.* **2001**, *40*, 2769. (j) Wietzke, R.; Mazzanti, M.; Latour, J.-M.; Pecaut, J. *Inorg. Chem.* **1999**, *38*, 3581. (k) Comba, P.; Zimmer, M. *Inorg. Chem.* **1994**, *33*, 5368. (l) Arana, C.; Yan, S.; Keshavarz, K. M.; Potts, K. T.; Abruña, H. D. *Inorg. Chem.* **1992**, *31*, 3680. (m) Pagenkopf, G. K.; Margerum, D. W. *Inorg. Chem.* **1968**, *7*, 2514. (n) Glaser, T.; Lügger, T.; Fröhlich, R. *Eur. J. Inorg. Chem.* **2004**, *2*, 394.

(3) (a) Polson, M. I. J.; Medlycott, E. A.; Hanan, G. S.; Mikelsons, L.; Taylor, N. J.; Watanabe, M.; Tanaka, Y.; Loiseau, F.; Passalacqua, R.; Campagna, S. *Chem.—Eur. J.* **2004**, *10*, 3640. (b) Gupta, N.; Grover, N.; Neyhart, G. A.; Singh, P.; Thorp, H. H. *Inorg. Chem.* **1993**, *32*, 310. (c) Paul, P.; Tyagi, B.; Bilakhiya, A. K.; Dastidar, P.; Suresh, E. *Inorg. Chem.* **2000**, 39, 14. (d) Metcalfe, C. M.; Spey, S.; Adams, H.; Thomas, J. A. *J. Chem. Soc., Dalton Trans.* **2002**, 4732. (e) Saji, T.; Aoyagui, S. *J. Electroanal. Chem.* **1980**, *110*, 329. (f) Tokel-Takvoryan, N. E.; Hemingway, R. E.; Bard, A. J. *J. Am. Chem. Soc.* **1973**, *95*, 6582. (g) Paul, P.; Tyagi, B.; Bhadbhade, M. M.; Suresh, E. *J. Chem. Soc., Dalton Trans.* **1997**, 2273. (h) Thomas, N. C.; Foley, B. L.; Rheingold, A. L. *Inorg. Chem.* **1988**, *27*, 3426. (i) Lin, C. T.; Bottcher, W.; Chou, M.; Creutz, C.; Sutin, N. *J. Am. Chem. Soc.* **1976**, *98*, 6536. (j) Lalrempuia, R.; Govindaswamy, P.; Mozharivskyj, Y. A.; Kollipara, M. R. *Polyhedron* **2004**, *23*, 1069. (k) Berger, R. M.; Holcombe, J. R. *Inorg. Chim. Acta* **1995**, *232*, 217. (l) Sharma, S.; Chandra, M.; Pandey, D. S. *Eur. J. Inorg. Chem.* **2004**, *17*, 3555. (m) Chandra, M.; Sahay, A. N.; Pandey, D. S.; Tripathi, R. P.; Saxena, J. K.; Reddy, V. J. M.; Puerta, M. C.; Valerga, P. *J. Organomet. Chem.* **2004**, *689*, 2256. (n) Chandra, M.; Sahay, A. N.; Pandey, D. S.; Puerta, M. C.; Valerga, P. *J. Organomet. Chem.* **2002**, *648*, 39. (o) Singh, A.; Singh, N.; Pandey, D. S. *J. Organomet. Chem.* **2002**, *642*, 48. (p) Chirayil, S.; Hegde, V.; Jahng, Y.; Thumme, R. P. *Inorg. Chem.* **1991**, *30*, 2821. (q) Chandra, M.; Sahay, A. N.; Pandey, D. S. *Indian J. Chem.* **2004**, *43A*, 323. (r) Berger, R. M.; Ellis, D. D. *Inorg. Chim. Acta* **1996**, *241*, 1.

(4) (a) Yenmez, I.; Specker, H. *Fresenius' Z. Anal. Chem.* **1979**, *296*, 140. (b) The Scifinder search shows the structure of one trinuclear Rh(3+) complex without any reference (registry no. 113006-61-4).

Scheme 1 [a]

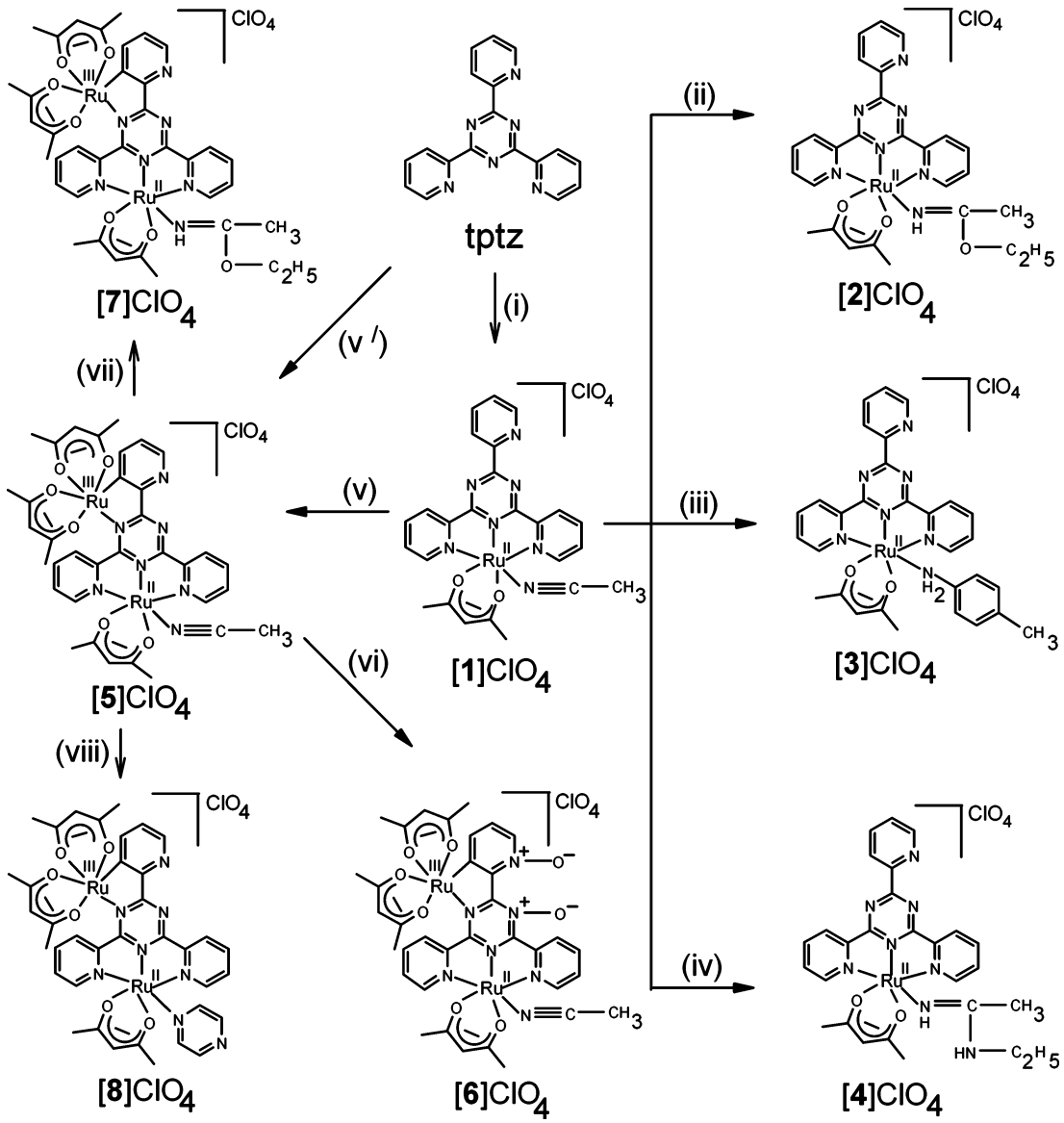

[a] (i) 1:1 $Ru(acac)_2(CH_3CN)_2$, EtOH, Δ; (ii) EtOH, Δ; (iii) $(CH_3)C_6H_4NH_2$, EtOH, Δ; (iv) $C_2H_5NH_2$, EtOH, Δ; (v) 1:1 $Ru(acac)_2(CH_3CN)_2$, EtOH, Δ; (v′) 1:2 $Ru(acac)_2(CH_3CN)_2$, EtOH, Δ; (vi) *m*-$ClC_6H_4CO_3H$, CH_2Cl_2, stir; (vii) EtOH, Δ; (viii) pyrazine, EtOH, Δ.

Alternatively, isomeric structure **I** or **II** (Chart 2) can also be drawn as a possible formulation for the dinuclear complex [**5**]ClO_4. However, motif **F** has been considered favorably as the metal−C bond because it originates from the available pendant pyridine ring of tptz instead of utilizing the already coordinated pyridine ring as in **I** or **II**.

Chart 2

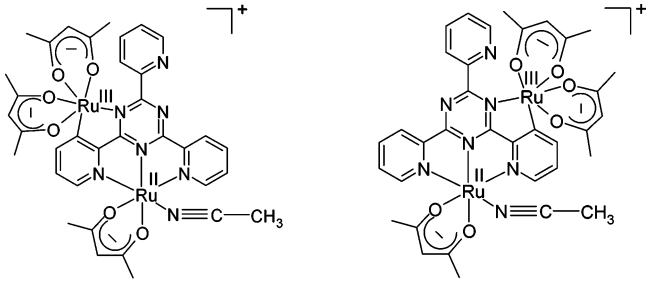

I **II**

The formation of an unprecedented cyclometalated N,C^- coordination mode of tptz with the second metal ion and subsequent stabilization of the mixed-valent $Ru^{II}Ru^{III}$ configuration in [**5**]ClO_4 (motif **F**) instead of the isovalent $Ru^{II}Ru^{II}$ state via the usual N,N bonding mode with the

(5) (a) Sarkar, B.; Patra, S.; Kaim, W.; Lahiri, G. K. *Angew. Chem., Int. Ed.* **2005**, *44*, 5655. (b) Kar, S.; Chanda, N.; Mobin, S. M.; Datta, A.; Urbanos, F. A.; Puranik, V. G.; Jimenez-Aparicio, R.; Lahiri, G. K. *Inorg. Chem.* **2004**, *43*, 4911. (c) Patra, S.; Sarkar, B.; Maji, S.; Fiedler, J.; Urbanos, F. A.; Jimenez-Aparicio, R.; Kaim, W.; Lahiri, G. K. *Chem.—Eur. J.* **2006**, *12*, 489. (d) Kar, S.; Chanda, N.; Mobin, S. M.; Urbanos, F. A.; Niemeyer, M.; Puranik, V. G.; Jimenez-Aparicio, R.; Lahiri, G. K. *Inorg. Chem.* **2005**, *44*, 1571. (e) Ghumaan, S.; Sarkar, B.; Patra, S.; Parimal, K.; van Slageren, J.; Fiedler, J.; Kaim, W.; Lahiri, G. K. *Dalton Trans.* **2005**, 706. (f) Patra, S.; Sarkar, B.; Ghumaan, S.; Fiedler, J.; Kaim, W.; Lahiri, G. K. *Dalton Trans.* **2005**, 754. (g) Patra, S.; Mondal, B.; Sarkar, B.; Niemeyer, M.; Lahiri, G. K. *Inorg. Chem.* **2003**, *42*, 1322. (h) Patra, S.; Sarkar, B.; Ghumaan, S.; Fiedler, J.; Kaim, W.; Lahiri, G. K. *Inorg. Chem.* **2004**, *43*, 6108. (i) Patra, S.; Miller, T. A.; Sarkar, B.; Niemeyer, M.; Ward, M. D.; Lahiri, G. K. *Inorg. Chem.* **2003**, *42*, 4707. (j) Patra, S.; Sarkar, B.; Mobin, S. M.; Kaim, W.; Lahiri, G. K. *Inorg. Chem.* **2003**, *42*, 6469.

Scheme 2

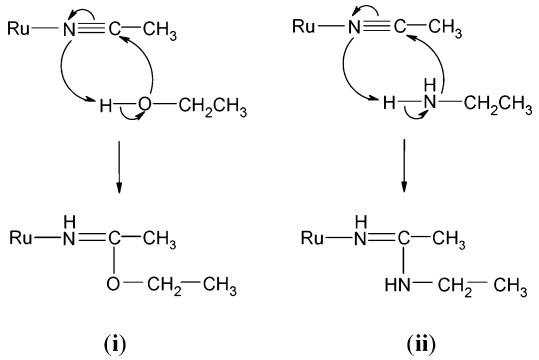

(**i**) (**ii**)

second metal (motif **C**) finds justification through its physical parameters such as conductivity, magnetic moment, and electron paramagnetic resonance (EPR) data (see below). This has also been further evidenced via the facile transformation of [**5**]ClO_4 to the N^+-O^- dinuclear derivative [**6**]ClO_4, upon reaction with *m*-chloroperbenzoic acid in CH_2Cl_2 (Scheme 1).[7]

The specific linkage of the π-accepting tptz unit with the Ru ion makes the nitrile function in [**1**]ClO_4 and [**5**]ClO_4 sufficiently electrophilic such that upon reactions with EtOH and ethylamine the corresponding iminoester ([**2**]ClO_4 and [**7**]ClO_4) and amidine ([**4**]ClO_4) derivatives, respectively (Scheme 1), have been formed via the nucleophilic addition routes, **i** and **ii** (Scheme 2).[8,9] The formation of [**2**]ClO_4 has been authenticated by its single-crystal X-ray structure (see later). However, the reaction of an aromatic primary amine, *p*-toluidine, with [**1**]ClO_4 resulted in a simple substituted product, [**3**]ClO_4 (Scheme 1), which has also been structurally characterized (see later).

The key step toward the amidine formation in [**4**]ClO_4 involves the nucleophilic attack of ^-NH-R on the carbonium center of the coordinated nitrile function as shown in route **ii (**Scheme 2). Thus, the electron-donating ethyl group as "R" in the amine fragment instead of the electron-withdrawing aryl group in *p*-toluidine facilitates the formation of active nucleophile ^-NH-R, which, in turn, leads to the yield of the amidine product [**4**]ClO_4. Though [**1**]ClO_4 can be easily transformed to [**4**]ClO_4, the reaction of ethyl- or methylamine with the corresponding dinuclear species [**5**]ClO_4 yielded materials that are insoluble in common solvents such as CH_3CN, CH_2Cl_2, C_6H_6, dimethylformamide, dimethyl sulfoxide, and H_2O. Thus, no attempt was made to further characterize the product. Unlike [**1**]ClO_4, the reaction of *p*-toluidine with [**5**]ClO_4 in a refluxing alcoholic medium mostly generated the iminoester derivative [**5**]ClO_4 along with a slight amount of the corresponding amine-substituted product (<5%).

Table 1. Mass Spectral Data in Acetonitrile for Complexes [**1**]ClO_4−[**8**]ClO_4

compound	*m*/*z*, obsd	correspondence	*m*/*z*, calcd
[**1**]ClO_4	554.09	[**1**]$^+$	554.08
	513.06	[**1**−CH_3CN]$^+$	513.06
[**2**]ClO_4	600.45	[**2**]$^+$	600.12
	513.34	[**2**−NHC(CH_3)(OEt)]$^+$	513.06
[**3**]ClO_4	620.23	[**3**]$^+$	620.13
	513.14	[**3**−(CH_3)$C_6H_4NH_2$]$^+$	513.06
[**4**]ClO_4	599.29	[**4**]$^+$	599.14
	513.19	[**4**−NHC(CH_3)(NHEt)]$^+$	513.06
[**5**]ClO_4	854.16	[**5**]$^+$	853.07
	812.13	[**5**−CH_3CN]$^+$	812.05
[**6**]ClO_4	887.19	[**6**]$^+$	885.06
	854.17	[**6**−2O]$^+$	853.07
[**7**]ClO_4	900.23	[**7**]$^+$	899.11
	854.18	[**7**−OEt]$^+$	854.08
	813.16	[**7**−NHC(CH_3)(OEt)]$^+$	812.05
[**8**]ClO_4	893.04	[**8**]$^+$	892.08
	813.01	[**8**−pyrazine]$^+$	812.05

It should be noted that under identical reaction conditions (Scheme 1) the activation of the nitrile functions in the precursor complex Ru(acac)$_2$(CH_3CN)$_2$ did not take place in the presence of alcohol or amine in an ethanolic medium. The presence of electronically rich $acac^-$ ligands in Ru(acac)$_2$(CH_3CN)$_2$ fails to make the coordinated nitrile functions electrophilic enough to participate in the acitivation processes (Scheme 2).

Attempts to synthesize pyrazine-bridged tetranuclear species from [**5**]ClO_4 in ethanol failed; a simple pyrazine-substituted product, [**8**]ClO_4, resulted instead. However, the same reaction of [**1**]ClO_4 with pyrazine in an ethanolic medium resulted in iminoester derivative [**2**]ClO_4.

The formations of 1:1 conducting diamagnetic mononuclear ([**1**]ClO_4−[**4**]ClO_4) and one-electron paramagnetic dinuclear ([**5**]ClO_4−[**8**]ClO_4) complexes have been confirmed by their elemental analyses (see the Experimental Section) and mass spectral data (Table 1 and Figures 1 and S1 in the Supporting Information). The single-crystal X-ray structures of [**1**]ClO_4, [**2**]ClO_4, and [**3**]ClO_4 have also been determined (see below).

Crystal Structures of [1]ClO_4·2H_2O, [2]ClO_4·2H_2O, and [3]ClO_4·2H_2O and the Formation of a Water Cluster in [2]ClO_4·2H_2O. The crystal structures of the cations of [**1**]ClO_4·2H_2O, [**2**]ClO_4·2H_2O, and [**3**]ClO_4·2H_2O are shown in Figures 2−4. Selected crystallographic and structural parameters are listed in Tables 2 and 3, respectively. In the complexes, tptz is coordinated to the Ru ion in the expected meridional fashion,[10] with the acac ligand in a cis position. The geometrical constraints due to the meridional binding of the tridentate tptz are reflected by the intraligand trans angles N1−Ru−N3 of 157.9(2), 157.76(16), and 158.2(2)° in [**1**]ClO_4, [**2**]ClO_4, and [**3**]ClO_4, respectively. The other two interligand trans angles N2−Ru−O1 and N7−Ru−O2 remain close to 180° for all three complexes. As in other

(6) (a) Chen, J.-L.; Zhang, X.-D.; Zhang, L.-Y.; Shi, L.-X.; Chen, Z.-N. *Inorg. Chem.* **2005**, *44*, 1037. (b) Minghetti, G.; Stoccoro, S.; Cinellu, M. A.; Soro, B.; Zucca, A. *Organometallics* **2003**, *22*, 4770. (c) Ward, M. D. *J. Chem. Soc., Dalton Trans.* **1994**, 3095.
(7) Wenkert, D.; Woodward, R. B. *J. Org. Chem.* **1983**, *48*, 283.
(8) (a) Nagao, H.; Hirano, T.; Tsuboya, N.; Shiota, S.; Mukaida, M.; Oi, T.; Yamasaki, M. *Inorg. Chem.* **2002**, *41*, 6267. (b) Bokach, N. A.; Kukushkin, V. Y.; Kuznetsov, M. L.; Garnovskii, D. A.; Natile, G.; Pombeiro, A. J. L. *Inorg. Chem.* **2002**, *41*, 2041.
(9) (a) Mondal, B.; Puranik, V. G.; Lahiri, G. K. *Inorg. Chem.* **2002**, *41*, 5831. (b) Chin, C. S.; Chong, D.; Lee, S.; Park, Y. J. *Organometallics* **2000**, *19*, 4043. (c) Chin, C. S.; Chong, D.; Lee, B.; Jeong, H.; Won, G.; Do, Y.; Park, Y. J. *Organometallics* **2000**, *19*, 638. (d) Anderes, B.; Lavallee, D. K. *Inorg. Chem.* **1983**, *22*, 3724. (e) Storhoff, B. N.; Lewis, H. C., Jr. *Coord. Chem. Rev.* **1977**, *23*, 1. (f) Cotton, F. A.; Wilkinson, G.; Murillo, C. A.; Bochmann, M. *Advanced Inorganic Chemistry*, 6th ed.; John Wiley and Sons: New York, 1999; pp 359−360.

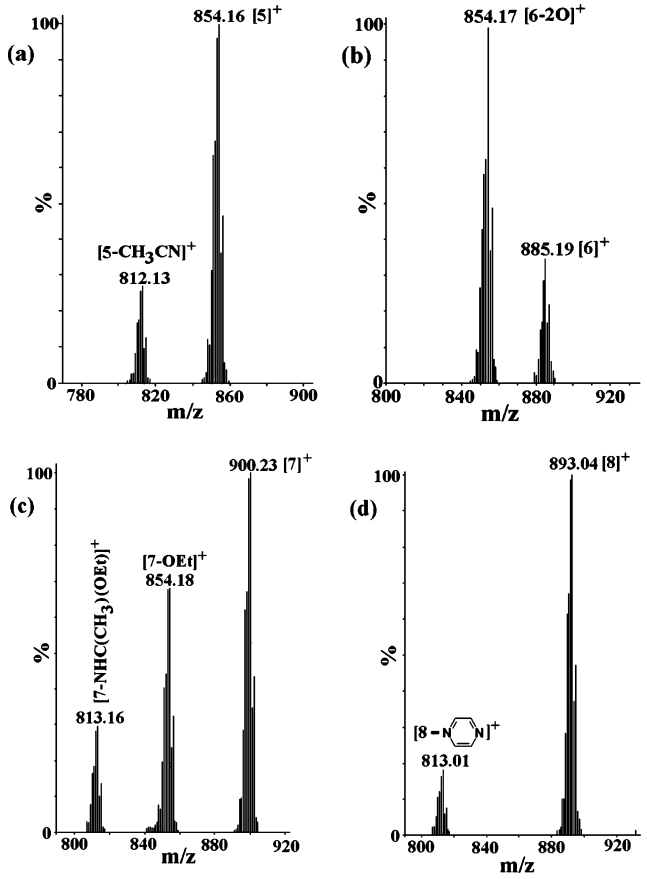

Figure 1. Electrospray mass spectra of (a) [**5**]ClO_4, (b) [**6**]ClO_4, (c) [**7**]ClO_4, and (d) [**8**]ClO_4 in CH_3CN.

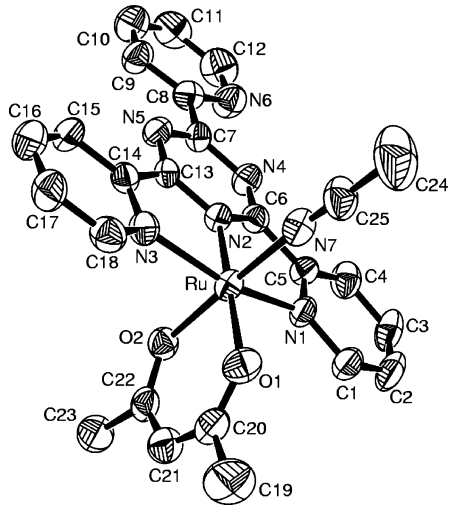

Figure 2. ORTEP diagram for the cation of [**1**]ClO_4·$2H_2O$. Ellipsoids are drawn at 50% probability.

Ru−tptz derivatives, the central Ru−N2(tptz) bond lengths of 1.913(5), 1.909(4), and 1.885(6) Å in [**1**]ClO_4, [**2**]ClO_4, and [**3**]ClO_4, respectively, are significantly shorter than the corresponding terminal Ru−N(tptz) distances, Ru−N1 [2.075(5), 2.081(4), and 2.064(6) Å] and Ru−N3 [2.088(5), 2.077(4), and 2.058(6) Å].[3] The pendant pyridine ring of tptz is

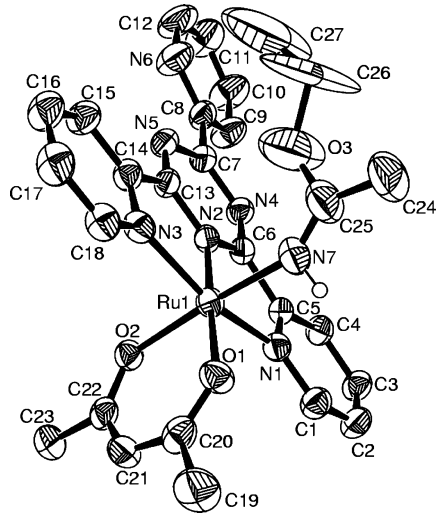

Figure 3. ORTEP diagram for the cation of [**2**]ClO_4·$2H_2O$. Ellipsoids are drawn at 50% probability.

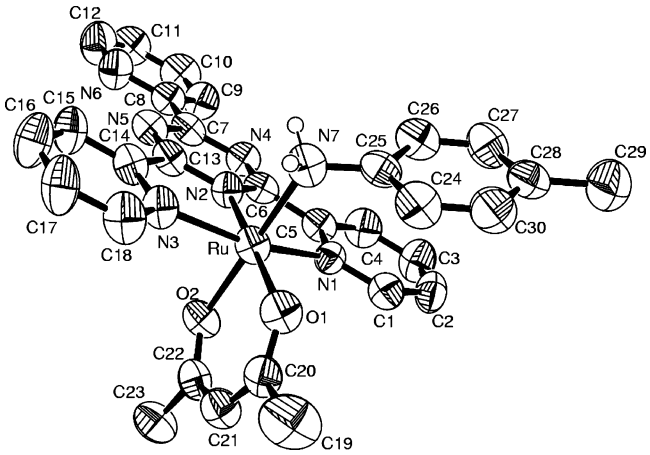

Figure 4. ORTEP diagram for the cation of [**3**]ClO_4·$2H_2O$ Ellipsoids are drawn at 50% probability.

Table 2. Crystallographic Data for [**1**]ClO_4, [**2**]ClO_4, and [**3**]ClO_4

	$C_{25}H_{22}ClN_7O_8Ru$	$C_{27}H_{32}ClN_7O_9Ru$	$C_{30}H_{28}N_7O_8Ru$
mol formula	[**1**]ClO_4·$2H_2O$	[**2**]ClO_4·$2H_2O$	[**3**]ClO_4·$2H_2O$
fw	685.02	735.12	751.11
radiation	Mo Kα	Mo Kα	Mo Kα
cryst sym	monoclinic	monoclinic	triclinic
space group	*P*21/*n*	*P*21/*n*	$P\bar{1}$
a (Å)	8.7920(12)	8.7430(11)	10.0010(7)
b (Å)	13.0460(11)	24.500(3)	13.1560(11)
c (Å)	24.771(3)	15.570(2)	14.0430(8)
α (deg)	90	90	103.831(6)
β (deg)	98.810(11)	97.896(2)	106.312(5)
γ (deg)	90	90	104.764(7)
V (Å^3)	2807.7(6)	3303.5(7)	1615.8(2)
Z	4	4	2
μ (mm^{-1})	0.715	0.615	0.628
T (K)	293(2)	293(2)	293(2)
D_{calcd} (g cm^{-3})	1.621	1.478	1.544
2*θ* range (deg)	3.32−49.82	3.12−50.00	3.40−49.9
E data (R_{int})	4924 (0.0390)	5815 (0.0648)	5673 (0.0612)
R1 [$I > 2\sigma(I)$]	0.0606	0.0557	0.0657
wR2 (all data)	0.1666	0.1610	0.1644
GOF	1.036	1.056	1.008

(10) (a) Patra, S.; Sarkar, B.; Ghumaan, S.; Patil, M. P.; Mobin, S. M.; Sunoj, R. B.; Kaim, W.; Lahiri, G. K. *Dalton Trans.* **2005**, 1188. (b) Chanda, N.; Paul, D.; Kar, S.; Mobin, S. M.; Datta, A.; Puranik, V. G.; Rao, K. K.; Lahiri, G. K. *Inorg. Chem.* **2005**, *44*, 3499. (c) Chanda, N.; Mobin, S. M.; Puranik, V. G.; Datta, A.; Niemeyer, M.; Lahiri, G. K. *Inorg. Chem.* **2004**, *43*, 1056. (d) Sarkar, S.; Sarkar, B.; Chanda, N.; Kar, S.; Mobin, S. M. Fiedler, J.; Kaim, W.; Lahiri, G. K. *Inorg. Chem.* **2005**, *44*, 6092.

Table 3. Selected Bond Distances (Å) and Angles (deg) for [**1**]ClO_4·$2H_2O$, [**2**]ClO_4·$2H_2O$, and [**3**]ClO_4·$2H_2O$

bond length/angle	[**1**]ClO_4·$2H_2O$	[**2**]ClO_4·$2H_2O$	[**3**]ClO_4·$2H_2O$
Ru−N2	1.913(5)	1.909(4)	1.885(6)
Ru−N7	2.031(6)	2.036(5)	2.145(6)
Ru−O1	2.066(5)	2.061(3)	2.054(5)
Ru−O2	2.039(4)	2.059(3)	2.043(5)
Ru−N3	2.088(5)	2.077(4)	2.058(6)
Ru−N1	2.075(5)	2.081(4)	2.064(6)
N7−C25	1.115(9)	1.165(8)	1.412(10)
C24−C25	1.438(11)	1.487(10)	1.384(11)
C25−O3		1.456(10)	
O3−C26		1.475(16)	
C26−C27		1.53(2)	
N2−Ru−N7	94.3(2)	96.03(17)	95.3(2)
N2−Ru−O1	178.9(2)	178.65(15)	178.9(3)
N7−Ru−O1	86.6(2)	83.03(16)	85.7(2)
N2−Ru−O2	88.18(19)	89.83(14)	87.4(2)
N7−Ru−O2	177.5(2)	174.14(17)	176.4(2)
O1−Ru−O2	90.97(18)	91.10(14)	91.6(2)
N2−Ru−N3	79.0(2)	78.84(16)	79.1(3)
N7−Ru−N3	90.8(2)	91.49(18)	89.1(3)
O1−Ru−N3	101.7(2)	102.13(15)	100.5(2)
O2−Ru−N3	89.70(19)	89.83(15)	89.0(2)
N2−Ru−N1	78.8(2)	78.92(16)	79.1(3)
N7−Ru−N1	92.0(2)	90.37(17)	92.7(2)
O1−Ru−N1	100.4(2)	100.10(15)	101.3(2)
O2−Ru−N1	88.46(19)	90.57(14)	90.1(2)
N3−Ru−N1	157.9(2)	157.76(16)	158.2(2)
Ru−N7−C25	174.9(7)	146.6(6)	118.5(5)

slightly nonplanar with respect to the triazine ring, and the dihedral angles are 5.25(0.46), 12.04(0.36), and 2.21(0.53)° for [**1**]ClO_4, [**2**]ClO_4, and [**3**]ClO_4, respectively. The much larger dihedral angle in [**2**]ClO_4 [12.04(0.36)°] compared to the other two complexes ([**1**]ClO_4 and [**3**]ClO_4) might be developed because of the H-bonding interaction between O10 of the eight-membered water cluster and N6 of the pendant pyridine ring of tptz in [**2**]ClO_4 (see later; Figure 5). The Ru−O(acac) bond distances agree well with the reported values.[5,11] The coordinated acetonitrile molecule in [**1**]ClO_4 is in its usual nearly linear mode with an N7−C25−C24 angle of 178.8(9)° and the N7−C25 triple-bond distance of 1.115(9) Å.[10d,12] The Ru−N7 single-bond distances in [**1**]ClO_4, [**2**]ClO_4, and [**3**]ClO_4 are 2.031(6), 2.036(5), and 2.145(6) Å, respectively. The expected sp, sp^2, and sp^3 hybridizations of N7 in [**1**]ClO_4, [**2**]ClO_4, and [**3**]ClO_4 are reflected in Ru−N7−C25 angles of 174.9(7), 146.6(6), and 118.5(5)°, respectively. However, the reasonable positive deviations of the Ru−N7−C25 angles from the idealized sp^2 (120°) and sp^3 (109.5°) angles in [**2**]ClO_4 and [**3**]ClO_4, respectively, suggest the partial sp and sp^2 characteristics of N7 possibly due to the contributions from the corresponding resonating forms. The RuN_4O_2 coordination sphere in the complexes exhibits a distorted octahedral geometry, as can be seen from the angles around the metal ions (Table 3). The change in the triple-bond characteristics of N7−C25 in [**1**]ClO_4 [1.115(9) Å] to double bond in [**2**]ClO_4 [1.165(8) Å] along with the corresponding change in the Ru−N7−C25 angle from linear to semibent geometry establishes the formation of an iminoester derivative in [**2**]ClO_4 via the activation of the nitrile function of [**1**]ClO_4 by ethanol, as shown in Scheme 2.

In [**1**]ClO_4, the intermolecular H-bonding interactions between the C15−H of one of the coordinated pyridine rings of tptz and the oxygen atom (O2) of the coordinated acac of a symmetry-related molecule have been observed. Moreover, one of the methyl hydrogens (C19−H19A) of acac is H-bonded to the oxygen atom (O5) of the ClO_4 molecule (Figure S2 and Table S1 in the Supporting Information).

The packing diagram of [**2**]ClO_4 reveals the formation of a beautiful eight-membered H_2O cluster having a chair conformation.[13] The cluster is formed via O8, O9, O10, and O11 of water molecules, and O8 of the water molecule is disordered. Further, O10 of the cluster is H-bonded to N6 of the pendant pyridyl ring of tptz. O10 is also H-bonded with O7 of the perchlorate ion, which, in turn, makes short (C−H- - - -O) contacts with the neighboring molecule, leading to a H-bonding network with a water cluster of the complex molecule. The H-bonding network is shown in Figure 5, and the distances are listed in Table 4. All O- - -O distances are below 3.0 Å (Table 4), confirming the stability of the H-bonding network (Figure 5).

^{1}H NMR Spectra. NMR spectral data of the diamagnetic complexes [**1**]ClO_4−[**4**]ClO_4 are set in the Experimental Section, and the representative spectra are shown in Figure 6. The calculated 12 and 16 aromatic protons for [**1**]ClO_4/[**2**]ClO_4/[**4**]ClO_4 and [**3**]ClO_4, respectively, appear in the range δ 7.0−9.0 as partially overlapping signals due to similar chemical shifts of many protons. The singlets corresponding to the C−H proton of acac and the CH_3 protons of acac/acetonitrile are observed near δ 5.0 and δ 2.6−1.2, respectively. The ethyl signals of OEt and NHEt for [**2**]ClO_4 and [**4**]ClO_4 appear at δ 3.4 (CH_2, quartet)/0.6 (CH_3, triplet) and δ 3.1 (CH_2, quintet because of additional coupling with the adjacent NH proton)/1.24 (CH_3, triplet), respectively. The coordinated NH proton of [**2**]ClO_4 is seen at δ 7.4 as a relatively broad singlet. However, the same for [**4**]ClO_4 displays a triplet profile at δ 7.6 because of the N nuclear spin $I = 1$.[14] The uncoordinated NH proton of [**4**]ClO_4 is observed at δ 4.6 as a broad singlet. The NH_2 protons of coordinated amine in [**3**]ClO_4 appear as doublet of doublets at δ 5.9 and 6.5.

Redox Processes and EPR Spectra. The Ru^{III}−Ru^{II} couple for the mononuclear complexes [**1**]ClO_4−[**4**]ClO_4 appears in the range of 0.77−0.51 V vs SCE, and it follows the order [**1**]ClO_4 ≫ [**2**]ClO_4 > [**3**]ClO_4 > [**4**]ClO_4 (Table 5 and Figure 7a). The stability of the Ru^{II} state decreases sharply upon moving from [**1**]ClO_4 (0.77 V) to [**2**]ClO_4 (0.59 V) based on the difference in the electron-withdrawing ability between the nitrile ($CH_3C{\equiv}N$) and imine [$NH{=}C(CH_3)$-OC_2H_5] functions. The two triazine-based successive one-

(11) Chao, G. K. J.; Sime, R. L.; Sime, R. J. *Acta Crystallogr. B* **1973**, *29*, 2845.
(12) Rasmussen, S. C.; Ronco, S. E.; Mlsna, D. A.; Billadeau, M. A.; Pennington, W. T.; Kolis, J. W.; Petersen, J. D. *Inorg. Chem.* **1995**, *34*, 821.
(13) (a) Ghosh, S. K.; Bharadwaj, P. K. *Inorg. Chem.* **2004**, *43*, 6887. (b) Ghosh, S. K.; Bharadwaj, P. K. *Angew. Chem., Int. Ed.* **2004**, *43*, 3577. (c) Ludwig, R. *Angew. Chem., Int. Ed.* **2001**, *40*, 1808. (d) Kar, S.; Sarkar, B.; Ghumaan, S.; Janardanan, D.; van Slageren, J.; Fiedler, J.; Puranik, V. G.; Sunoj, R. B.; Kaim, W.; Lahiri, G. K. *Chem.—Eur. J.* **2005**, *11*, 4901. (e) Head-Gordon, T.; Hura, G. *Chem. Rev.* **2002**, *102*, 2651. (f) Keutsch, F. N.; Cruzan, J. D.; Saykally, R. J. *Chem. Rev.* **2003**, *103*, 2533.
(14) Keerthi, K. D.; Santra, B. K.; Lahiri, G. K. *Polyhedron* **1998**, *17*, 1387.

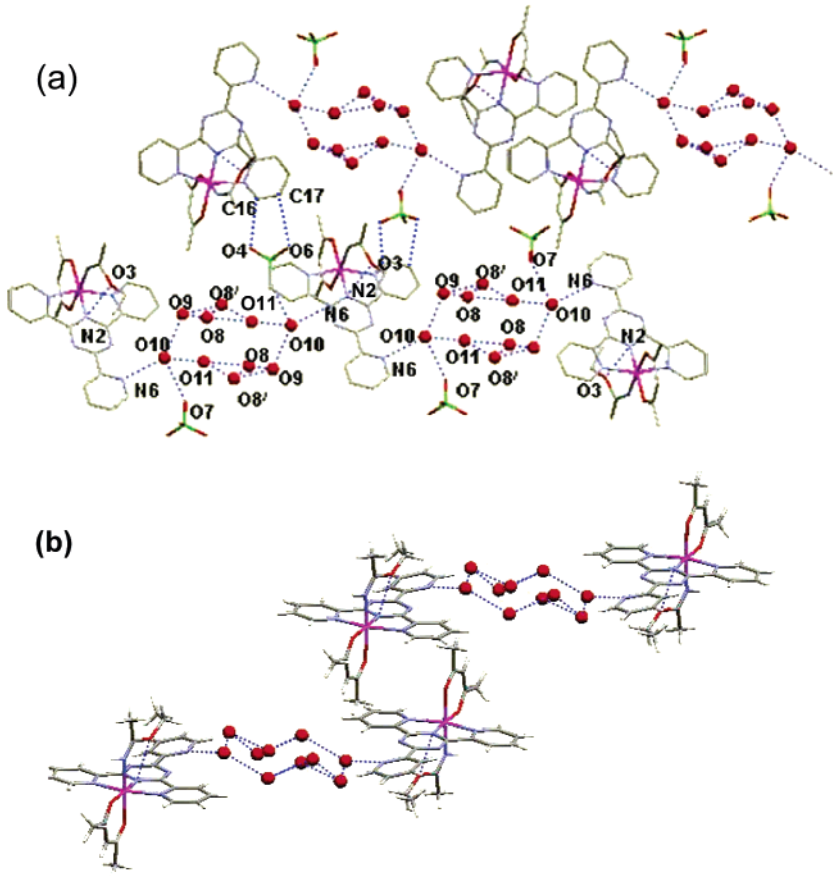

Figure 5. (a) H-bonding network in [**2**]ClO_4·$2H_2O$ and (b) chair conformation of a water cluster in [**2**]ClO_4·$2H_2O$ down the *b* axis.

Table 4. Distances Relevant to H Bonds (Å) in [**2**]ClO_4·$2H_2O$

atom 1	atom 2	symmetry 1	symmetry 2	distance (Å)
O3	N2	*x*, *y*, *z*	*x*, *y*, *z*	2.929
N6	O10	*x*, *y*, *z*	1 − *x*, −*y*, 1 − *z*	2.880
O7	O10	1 − *x*, −*y*, 1 − *z*	1 − *x*, −*y*, 1 − *z*	2.871
O7	O10	1 + *x*, *y*, 1 + *z*	1 + *x*, *y*, 1 + *z*	2.871
O3	N2	2 − *x*, −*y*, 2 − *z*	2 − *x*, −*y*, 2 − *z*	2.929
N6	O10	2 − *x*, −*y*, 2 − *z*	1 + *x*, *y*, 1 + *z*	2.880
O9	O10	*x*, *y*, *z*	1 − *x*, −*y*, 1 − *z*	2.817
O9	O8	*x*, *y*, *z*	*x*, *y*, *z*	2.099
O9	O8′	*x*, *y*, *z*	*x*, *y*, *z*	2.913
O8	O11	*x*, *y*, *z*	1 + *x*, *y*, 1 + *z*	2.747
O8′	O11	*x*, *y*, *z*	1 + *x*, *y*, 1 + *z*	2.210
O10	O11	1 − *x*, −*y*, 1 − *z*	1 − *x*, −*y*, 1 − *z*	3.015

electron reductions are observed in the range of −0.9 to −1.8 V (Table 5). However, in the complex [**3**]ClO_4, the second triazine-based reduction has surprisingly appeared at a much lower potential, −1.27 V (Table 5). The ligand-centered (tptz) reduction process has been supported by the free-radical-type EPR signal at $\langle g \rangle = 2.054$, obtained from the electrochemically generated one-electron-reduced species **1**, at 77 K (Figure 8a). The appearance of a slightly axial-type EPR spectrum ($\Delta g = 0.08$) suggests a partial metal contribution in the singly occupied lowest unoccupied molecular orbital (LUMO). The expected N hyperfine splitting ($I = 1$ for ^{14}N) has not been resolved.[15]

The dinuclear complex [**5**]ClO_4 exhibits two successive $Ru^{III}-Ru^{II}$ couples at 0.20 (couple I) and 0.88 V (couple II) vs SCE (Table 5 and Figure 7b). The first couple at 0.20 V is associated with the reduction of the Ru^{III} center encompassing an electronically rich two $acac^-$ and carbanion (C^-)

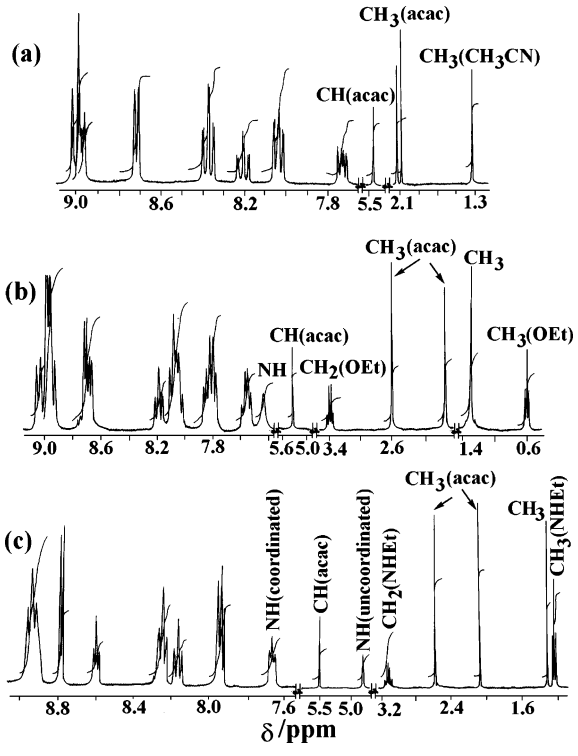

Figure 6. ^1H NMR spectra of (a) [**1**]ClO_4 in $CDCl_3$, (b) [**2**]ClO_4, and (c) [**4**]ClO_4 in $(CD_3)_2SO$.

based $\{Ru^{III}(O_2^-,acac)_2(N,C^-,tptz)\}$ chromophore, whereas the couple at higher potential (couple II) originates from the oxidation of the Ru^{II} center with a $\{Ru^{II}O_2(acac^-)$-

Table 5. Electrochemical[a] and EPR[b] Data

	$E°_{298}$ (V) (ΔE_p (mV))									
compd	$Ru^{III}-Ru^{II}$ couple	$Ru^{III} \rightarrow Ru^{IV}$	K_c[d]	ligand reduction	μ_B	g_1	g_2	g_3	$\langle g \rangle$[e]	Δg[f]
[**1**]ClO_4	0.77 (90)			−0.99 (80), −1.72 (90)						
[**2**]ClO_4	0.59 (90)			−1.05 (90), −1.72 (90)						
[**3**]ClO_4	0.54 (120)			−0.91 (60), −1.27 (110)						
[**4**]ClO_4	0.51 (80)			−1.07 (100), −1.77 (120)						
[**5**]ClO_4	0.20 (80), 0.88 (80)	1.57[c]	3.4×10^{11}	−0.97 (100)	2.2	2.35	2.23	1.85	2.15	0.5
[**6**]ClO_4	0.22 (90), 0.93 (90)	1.63[c]	1.1×10^{12}	−0.93 (110)	1.9	2.34	2.18	1.84	2.13	0.5
[**7**]ClO_4	0.18 (120), 0.73 (60)	1.57[c]	2×10^9	−0.94 (70)	1.9	2.36	2.24	1.86	2.16	0.5
[**8**]ClO_4	0.18 (90), 0.86 (90)	1.57[c]	3.4×10^{11}	−0.92 (70)	2.0	2.38	2.21	1.81	2.15	0.56

[a] In CH_3CN vs SCE. [b] In $CHCl_3$ at 77 K. [c] Irreversible. [d] $RT \ln K_c = nF(\Delta E)$. [e] $\langle g \rangle = [1/3(g_1^2 + g_2^2 + g_3^2)]^{1/2}$. [f] $\Delta g = g_1 - g_3$.

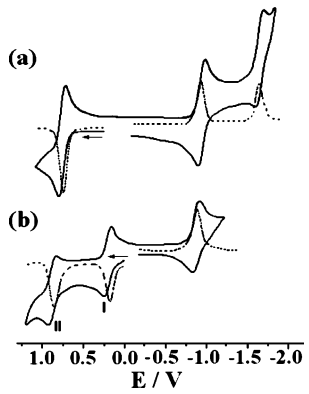

Figure 7. Cyclic voltammograms (—) and differential pulse voltammograms (- - -) in CH_3CN of (a) [**1**]ClO_4 and (b) [**5**]ClO_4.

$N_3(tptz)N(CH_3CN)^+$} chromophore.[5e] The low $Ru^{III}-Ru^{II}$ potential of couple I (0.20 V) facilitates the stabilization of the mixed-valent state in [**5**]ClO_4 under atmospheric conditions. The corresponding irreversible $Ru^{III} \rightarrow Ru^{IV}$ process appears at 1.57 V (Table 5). However, the same corresponding to couple II has not been detected until the solvent cutoff point (2 V). The oxidation potential of the Ru^{II} center in [**5**]ClO_4 (couple II) is about 100 mV greater than that of the corresponding mononuclear derivative, [**1**]ClO_4. The presence of the second metal ion in the Ru^{III} state via the involvement of negatively charged $tptz^-$ and $acac^-$ ligands in [**5**]ClO_4 increases the stability of the adjacent Ru^{II} center further compared to that in [**1**]ClO_4. The 680 mV separation in potential between the successive $Ru^{III}-Ru^{II}$ couples (couple II−couple I) in [**5**]ClO_4 is due to the consequences of two simultaneously operating factors: (i) built-in donor center asymmetry around the metal ions [{$Ru^{III}(O_2^-,acac)_2$-$(N,C^-,tptz)$} and {$Ru^{II}O_2(acac^-)N_3(tptz)N(CH_3CN)^+$}] and (ii) bridging ligand (tptz) mediated intermetallic coupling process.[5e,16] The resulting comproportionation constant (K_c) value of the mixed-valent $Ru^{III}Ru^{II}$ state is 3.4×10^{11} [calculated using the relation $RT \ln K_c = nF(\Delta E)$[17]]. For [**7**]$ClO_4$ and [**8**]ClO_4, the potentials corresponding to the

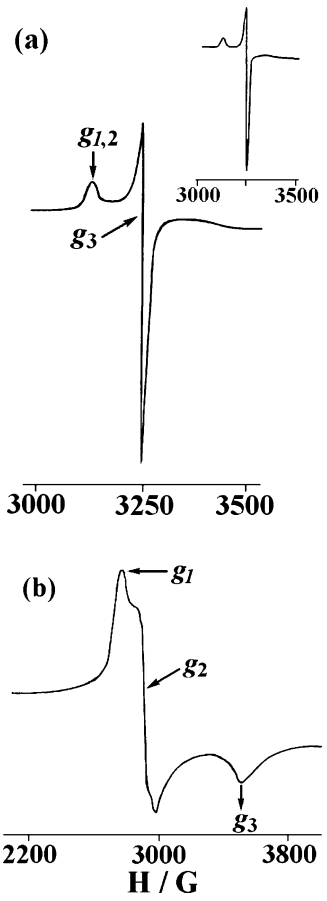

Figure 8. EPR spectra of (a) electrogenerated **1** in CH_3CN/0.1 M Et_4NClO_4 (inset shows the spectrum of electrogenerated **5** in CH_3CN/0.1 M Et_4NClO_4) and (b) [**7**]ClO_4 in $CHCl_3$ at 77 K.

redox processes involving the Ru^{III} center ($Ru^{III}-Ru^{II}$, couple I, and $Ru^{III} \rightarrow Ru^{IV}$) remain almost close to those of [**5**]ClO_4 (Table 5). However, relative to [**5**]ClO_4, the stability of the Ru^{II} center (couple II) in [**7**]ClO_4 decreases reasonably (0.88 V in [**5**]ClO_4 vs 0.73 V in [**7**]ClO_4), as has been observed in the mononuclear systems, [**1**]ClO_4 vs [**2**]ClO_4. On the other hand, the $Ru^{II}-Ru^{III}$ potential (couple II) for the pyrazine derivative [**8**]ClO_4 appears to be very close to that of the parent acetonitrile complex [**5**]ClO_4 (Table 5). The K_c values for [**7**]ClO_4 and [**8**]ClO_4 are calculated as 2×10^9 and 3.4×10^{11}, respectively. The variation in K_c based on the electronic nature of the sixth ligands associated with the Ru^{II} center among similar dinuclear complexes, K_c of [**8**]ClO_4 (pyrazine) = [**5**]ClO_4 (CH_3CN) ≫ [**7**]ClO_4 [$NH{=}C(CH_3)OC_2H_5$] (Table 5), signifies that, in addition

(15) (a) Sarkar, B.; Laye, R. H.; Mondal, B.; Chakraborty, S.; Paul, R. L.; Jeffery, J. C.; Puranik, V. G.; Ward, M. D.; Lahiri, G. K. *J. Chem. Soc., Dalton Trans.* **2002**, 2097. (b) Chanda, N.; Laye, R. H.; Chakraborty, S.; Paul, R. L.; Jeffery, J. C.; Ward, M. D.; Lahiri, G. K. *J. Chem. Soc., Dalton Trans.* **2002**, 3496. (c) Bock, H.; Jaculi, D. Z.; Naturforsch, B. *Anorg. Chem., Org. Chem.* **1991**, *46*, 1091. (d) Ward, M. D. *Inorg. Chem.* **1996**, *35*, 1712.
(16) Chakraborty, S.; Laye, R. H.; Munshi, P.; Paul, R. L.; Ward, M. D.; Lahiri, G. K. *J. Chem. Soc., Dalton Trans.* **2002**, 2348.
(17) Creutz, C. *Prog. Inorg. Chem.* **1983**, *30*, 1.

Table 6. UV−Visible Spectral Data for Complexes [**1**]ClO_4−[**8**]ClO_4 in Acetonitrile

compd	λ_{max} (nm) (ϵ (M^{-1} cm^{-1}))
[**1**]ClO_4	620 (4680),[a] 522 (11 340), 366 (11 000), 280 (38 280), 202 (41 890)
[**2**]ClO_4	663 (3180),[a] 538 (11 900), 384 (9990), 280 (40 760), 208 (28 700)
[**3**]ClO_4	668 (2530),[a] 542 (9310), 388 (7850), 278 (36 260), 202 (31 630)
[**4**]ClO_4	694 (3620),[a] 554 (12 800), 398 (10 670), 279 (37 720), 248 (27 690), 206 (34 900)
[**5**]ClO_4	624 (9380), 544 (6940), 384 (12 320), 276 (40 160), 200 (47 650)
[**6**]ClO_4	560 (5970), 370 (5960), 280 (22 500), 202 (57 900)
[**7**]ClO_4	624 (13 280), 562 (9200), 390 (14 260), 276 (47 650), 200 (49 600)
[**8**]ClO_4	628 (11 820), 558 (7920), 392 (16 050), 278 (39 350), 198 (40 160)

[a] Shoulder.

to the tptz-mediated intermetallic coupling process, the factor related to donor center asymmetry on the two Ru ions also contributes significantly to the observed fairly large K_c value.[5e,16]

One triazine-based reduction has also been detected for all of the dinuclear complexes. However, the expected second triazine-based reduction has not been observed within the experimental potential range of −2.0 V, possibly because of the effect of the additional negative charge associated with the anionic tptz ligand in the dinuclear complexes. The reduction potential is found to be slightly lower than that of the corresponding mononuclear derivatives (Table 5) because of the additional binding of tptz with the second Ru ion in the Ru^{III} state. The electrochemically generated tptz-reduced species **5** exhibits a free-radical-type EPR spectrum at 77 K ($\langle g \rangle = 2.058$ and $\Delta g = 0.08$) with a partial metal contribution, as has been observed earlier in the case of **1** (Figure 8a, inset).

Mixed-valent $Ru^{II}Ru^{III}$ dinuclear complexes [**5**]ClO_4−[**8**]ClO_4 exhibit magnetic moments corresponding to those of one unpaired electron and display rhombic EPR spectra at 77 K (Table 5 and Figure 8b). The large g anisotropy [Δg ($g_1 - g_3$) ∼ 0.5; Table 5] signifies a considerably distorted octahedral arrangement around the metal ion, as can be expected from the mixed {$Ru^{III}O_4NC$} coordination environment.[18] The average g factor of $\langle g \rangle \sim 2.15$ is derived from $\langle g \rangle = [1/3(g_1^2 + g_2^2 + g_3^2)]^{1/2}$ (Table 5).[5f]

Electronic Spectra. Mononuclear complexes [**1**]ClO_4−[**4**]ClO_4 exhibit multiple intense transitions in the UV−visible region due to the presence of different acceptor levels (Table 6 and Figure 9a). The lowest-energy band near 500 nm is associated with a broad shoulder at the further lower-energy part. The visible-region bands near 500 and 400 nm can be tentatively assigned as metal-to-ligand charge-transfer (MLCT) transitions involving the Ru^{II} ion and the triazine- and acac-based acceptor levels, respectively.[3,5] The MLCT bands expectedly blue-shifted with the increasing stability of the Ru^{II} state, [**1**]ClO_4 > [**2**]ClO_4 > [**3**]ClO_4 > [**4**]ClO_4, as has been observed in their redox potentials (Table 5). The UV-region strong transitions are believed to originate from the intraligand $\pi-\pi^*$/n−π^* transitions.

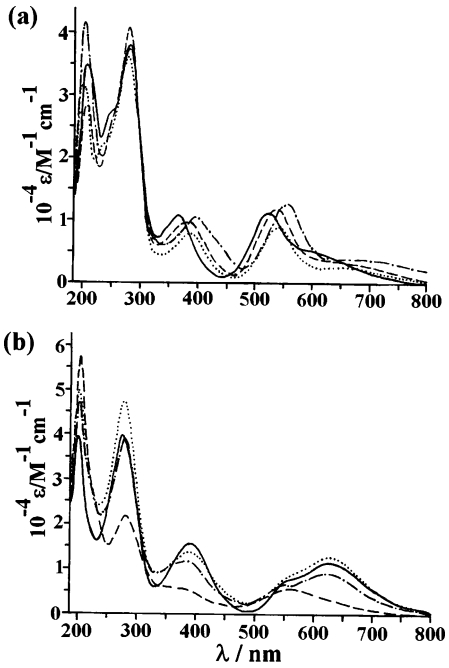

Figure 9. UV−visible spectra in CH_3CN of (a) [**1**]ClO_4 (—), [**2**]ClO_4 (− − −), [**3**]ClO_4 (···), and [**4**]ClO_4 (−·−) and (b) [**5**]ClO_4 (−·−), [**6**]ClO_4 (− − −), [**7**]ClO_4 (···), and [**8**]ClO_4 (—).

The dinuclear complexes [**5**]ClO_4, [**7**]ClO_4, and [**8**]ClO_4 exhibit two intense CT transitions in the visible region near 600 and 400 nm. The lowest-energy transition near 600 nm is associated with an overlapping band near 550 nm (Figure 9b and Table 6). Though the position of the lowest-energy band remains almost invariant, the next-higher-energy band is seen to be red-shifted from 544 to 562 to 558 nm while moving from [**5**]ClO_4 → [**7**]ClO_4 → [**8**]ClO_4. Thus, the lowest-energy bands near 600 nm may be considered as ligand-to-metal CT (LMCT) transitions involving the Ru^{III} center having an identical RuO_4NC chromophore in all three complexes and tptz. The next-higher-energy bands near 550 nm may thus be assumed as MLCT transitions involving the Ru^{II} center with varying sixth ligands and tptz similar to the Ru^{II}-based MLCT transitions in the corresponding mononuclear complexes [**1**]ClO_4 and [**2**]ClO_4, which also appear near 550 nm. The intense band near 400 nm may be considered as an acac-based MLCT or LMCT transition. Ligand-based CT transitions are also observed in the UV region. The same Ru^{III}- and Ru^{II}−tptz-based LMCT and MLCT transitions in [**6**]ClO_4, however, appear as an overlapping broad band at a relatively higher energy of 560 nm, and the acac-based transition is observed at 370 nm. Therefore, the introduction of $-N^+-O^-$ units in the tptz framework of [**6**]ClO_4 enhances the energy gap between the donor and acceptor levels compared to that in the other dinuclear complexes.

The mixed-valent $Ru^{II}Ru^{III}$ complexes [**5**]ClO_4−[**8**]ClO_4 failed to show expected intervalence CT (IVCT) transitions up to 2000 nm in spite of strong electrochemical coupling ($K_c = 10^9-10^{12}$). A similar situation of high K_c but no IVCT

(18) (a) Poppe, J.; Moscherosch, M.; Kaim, W. *Inorg. Chem.* **1993**, *32*, 2640. (b) Bag, N.; Lahiri, G. K.; Basu, P.; Chakravorty, A. *J. Chem. Soc., Dalton Trans.* **1992**, 113.

bands in the typically expected near-IR region in mixed-valent states of Ru−acac-based dinuclear and trinuclear complexes has also been reported recently.[5c,f,h] Mixed-valent species with high K_c values but without any IVCT bands are simply puzzling. Therefore, we prefer to assume that the intensity of the IVCT band ($\epsilon < 20$) is too weak to be detected under the present experimental conditions. Alternatively, it may also be considered that the expected IVCT transition has been hidden in the intense CT band near 600 nm. The cyclic voltammetric and EPR results have already indicated a strong interaction between the metals and the negatively charged tptz$^-$, raising the energies of Ru−tptz$^-$ mixed occupied orbitals while that of the acceptor LUMO-(tptz) remains constant.[19]

Electrochemically oxidized mononuclear Ru^{III} and dinuclear $Ru^{III}Ru^{II}$ derivatives were found to be unstable at the coulometric time scale at 298 K.

Conclusion

In summary, the Ru precursor complex $Ru(acac)_2(CH_3CN)_2$ facilitates (i) the formation of an unprecedented bridging motif of tptz (motif **F**) and (ii) the subsequent stabilization of a mixed-valent $Ru^{II}Ru^{III}$ configuration in the native state of [**5**]ClO_4−[**8**]ClO_4. Moreover, the nitrile function associated with the Ru^{II} center in the mononuclear [**1**]ClO_4 as well as dinuclear [**5**]ClO_4 complexes has been activated in the presence of protic nucleophiles such as alcohol and alkylamine to yield the corresponding iminoester ([**2**]ClO_4 and [**7**]ClO_4) and amidine [**4**]ClO_4 derivatives, respectively. The mixed-valent dinuclear complexes ([**5**]ClO_4−[**8**]ClO_4) failed to show the expected IVCT transitions in the typical near-IR region in spite of reasonably high electrochemical coupling ($K_c = 10^9-10^{12}$).

Experimental Section

The starting complex $Ru(acac)_2(CH_3CN)_2$ was prepared according to the reported procedure.[20] 2,4,6-Tris(2-pyridyl)-1,3,5-triazine (tptz) was purchased from Aldrich (Madison, WI). Other chemicals and solvents were reagent grade and were used as received. For spectroscopic and electrochemical studies, high-performance liquid chromatography grade solvents were used.

UV−visible spectral studies were performed on a Jasco 570 spectrophotometer. A Perkin-Elmer Lambda-950 instrument was used to check the possible near-IR transitions. Fourier transform (FT) IR spectra were obtained on a Nicolet spectrophotometer with samples prepared as KBr pellets. The solution electrical conductivity was checked using a Systronic 305 conductivity bridge. ^{1}H NMR spectra were obtained with a 300-MHz Varian FT spectrometer. The EPR measurements were made with a Varian model 109C E-line X-band spectrometer fitted with a quartz Dewar for 77 K. Cyclic voltammetric, differential pulse voltammetric, and coulometric measurements were carried out using a PAR model 273A electrochemistry system. Platinum wire working and auxiliary electrodes and an aqueous saturated calomel reference electrode (SCE) were used in a three-electrode configuration. The supporting electrolyte was Et_4NClO_4, and the solute concentration was $\sim 10^{-3}$ M. The half-wave potential $E°_{298}$ was set equal to $0.5(E_{pa} + E_{pc})$, where E_{pa} and E_{pc} are anodic and cathodic cyclic voltammetric peak potentials, respectively. A platinum wire−gauze working electrode was used in coulometric experiments. All experiments were carried out under a N_2 atmosphere. The elemental analysis was carried out with a Perkin-Elmer 240C elemental analyzer. Positive ion electrospray mass spectra were recorded on a Micromass Q-ToF mass spectrometer. The magnetic susceptibility was measured with a Faraday balance (Cahn Instruments Inc., serial no. 76240).

Synthesis of [1]ClO_4. The precursor complex $Ru(acac)_2(CH_3CN)_2$ (100 mg, 0.26 mmol) and the ligand tptz (81.9 mg, 0.26 mmol) in a 1:1 molar ratio were dissolved in 20 mL of ethanol, and the mixture was heated to reflux for 10 h under a N_2 atmosphere. The solid mass thus obtained upon evaporation of the solvent was dissolved in a minimum volume of CH_3CN. To this was added an excess aqueous $NaClO_4$ solution, and the mixture was kept in deep freeze overnight. It was then filtered, and the solid mass was washed with ice-cold water followed by cold ethanol and dried under vacuum. It was then purified using a neutral alumina column. Initially, a red compound corresponding to $Ru(acac)_3$ was eluted by CH_2Cl_2−CH_3CN (20:1), followed by a violet compound corresponding to [**1**]ClO_4, which was eluted with CH_2Cl_2−CH_3CN (15:1). Evaporation of the solvent mixture yielded the pure compound [**1**]ClO_4. Yield: 70 mg (41%). Anal. Calcd (found) for [**1**]ClO_4 ($RuC_{25}H_{22}N_7O_6Cl$): C, 45.94 (45.64); H, 3.40 (3.60); N, 15.01 (14.80). Molar conductivity [Λ_M (Ω^{-1} cm^2 M^{-1})] in acetonitrile at 298 K: 112. IR [$\nu(ClO_4^-)$/cm^{-1}]: 1097, 619. ^{1}H NMR [$(CD_3)_2SO$, δ (*J*, Hz)]: 9.0 (d, 7.2), 8.98 (multiplet, chemical shift range 8.94−9.0 ppm), 8.72 (d, 4.8), 8.37 (t, 7.9, 7.6), 8.2 (t, 7.7, 7.9), 8.04 (t, 6.0, 6.8), 7.73 (t, 6.0, 7.5), 5.45 (s, CH(acac)), 2.13, 2.08 (s, CH_3(acac)), 1.32 (s, $CH_3(CH_3CN)$).

Synthesis of [2]ClO_4. [**1**]ClO_4 (50 mg, 0.076 mmol) was refluxed in ethanol for 36 h under a N_2 atmosphere. The initial violet color of the solution gradually changed to purple. The solvent was removed under reduced pressure, and the residue was purified using a neutral alumina column. A purple compound corresponding to [**2**]ClO_4 was eluted by CH_2Cl_2−CH_3CN (5:1). Evaporation of the solvent mixture yielded the pure compound [**2**]ClO_4. Yield: 25 mg (46%). Anal. Calcd (found) for [**2**]ClO_4 ($RuC_{27}H_{28}N_7O_7Cl$): C, 46.35 (46.50); H, 4.04 (4.20); N, 14.02 (14.30). Molar conductivity [Λ_M (Ω^{-1} cm^2 M^{-1})] in acetonitrile at 298 K: 102. IR [$\nu(ClO_4^-)$/cm^{-1}]: 1121, 624. ^{1}H NMR [$CDCl_3$, δ (*J*, Hz)]: δ 9.04 (d, 7.8), 8.93 (multiplet), 8.69 (multiplet), 8.18 (t, 7.5, 7.8), 8.06 (multiplet), 7.82 (multiplet), 7.55 (multiplet), 7.44 (s, NH), 5.33 (s, CH(acac)), 3.38 (q, 7.2, 6.9, 7.2, CH_2), 2.62, 1.96 (s, CH_3(acac)), 1.30 (s, $CH_3(CH_3CN)$), 0.60 (t, 6.9, 6.9, CH_3).

Synthesis of [3]ClO_4. [**1**]ClO_4 (50 mg, 0.076 mmol) and *p*-toluidine (8.21 mg, 0.076 mmol) were dissolved in 20 mL of ethanol, and the mixture was heated to reflux for 8 h under a N_2 atmosphere. The solvent was removed under reduced pressure, and the residue was purified using a neutral alumina column. The complex [**3**]ClO_4 was eluted by CH_2Cl_2−CH_3CN (3:1). Evaporation of the solvent mixture yielded the pure compound [**3**]ClO_4. Yield: 16 mg (30%). Anal. Calcd (found) for [**3**]ClO_4 ($RuC_{30}H_{28}N_7O_6Cl$): C, 50.06 (50.34); H, 3.92 (4.12); N, 13.63 (13.84). Molar conductivity [Λ_M (Ω^{-1} cm^2 M^{-1})] in acetonitrile at 298 K: 130. IR [$\nu(ClO_4^-)$/cm^{-1}]: 1087, 619. ^{1}H NMR [$CDCl_3$, δ (*J*, Hz)]: δ 8.95 (multiplet), 8.66 (d, 6.0), 8.46 (d, 7.5), 8.16 (t, 9.0, 6.0), 8.0 (multiplet), 7.82 (t, 6.0, 9.0), 7.75 (multiplet), 7.62 (multiplet), 7.54 (multiplet), 6.47 (d, 9.0, NH_2), 5.95 (d, 9.0, NH_2), 5.34 (s, CH(acac)), 2.62, 2.53 (s, CH_3(acac)), 1.98 (s, CH_3).

(19) Chanda, N.; Sarkar, B.; Kar, S.; Fiedler, J.; Kaim, W.; Lahiri, G. K. *Inorg. Chem.* **2004**, *43*, 5128.
(20) Kobayashi, T.; Nishina, Y.; Shimizu, K.; Satô, G. P. *Chem. Lett.* **1988**, 1137.

Synthesis of [4]ClO_4. [**1**]ClO_4 (50 mg, 0.076 mmol) and a 70% aqueous solution of ethylamine in excess (1 mL) were refluxed in ethanol for 4 h under a N_2 atmosphere. The solvent was removed under reduced pressure, and the residue was purified using a neutral alumina column. A bluish-violet compound corresponding to [**4**]ClO_4 was eluted by $CH_2Cl_2-CH_3CN$ (4:1). Evaporation of the solvent mixture yielded the pure compound [**4**]ClO_4. Yield: 20 mg (37%). Anal. Calcd (found) for [**4**]ClO_4 ($RuC_{27}H_{29}N_8O_6Cl$): C, 46.41 (46.65); H, 4.19 (4.36); N, 16.05 (16.35). Molar conductivity [Λ_M (Ω^{-1} cm^2 M^{-1})] in acetonitrile at 298 K: 130. IR [$\nu(ClO_4^-)$/cm^{-1}]: 1107, 629. ^{1}H NMR [$(CD_3)_2SO$, δ (*J*, Hz)]: δ 8.94 (multiplet), 8.79 (d, 5.0), 8.60 (t, 5.2, 5.6), 8.25 (t, 9.2, 8.0), 8.16 (t, 8.0, 6.4), 7.94 (t, 8.0, 8.0), 7.67 (t, coordinated NH), 5.51 (s, CH(acac)), 4.78 (s, uncoordinated NH), 3.12 (quintet, 7.2, 6.0, 8.0, 8.0, CH_2), 2.57, 2.07 (s, CH_3(acac)), 1.32 (s, CH_3), 1.24 (t, 7.2, 7.2, CH_3).

Synthesis of [5]ClO_4. The precursor complex Ru(acac)$_2$-(CH_3CN)$_2$ (100 mg, 0.26 mmol) and tptz (40 mg, 0.13 mmol) in a 2:1 molar ratio were dissolved in 20 mL of ethanol, and the mixture was heated to reflux for 10 h. The initial orange color of the solution gradually changed to bluish-green. The bluish-green mass thus obtained upon evaporation of the solvent was dissolved in a minimum volume of CH_3CN. To this was added an excess aqueous $NaClO_4$ solution, and the mixture was kept in deep freeze overnight. It was then filtered, and the solid mass was washed with ice-cold water followed by cold ethanol and diethyl ether and dried under vacuum. It was then purified using a neutral alumina column. Initially, a red compound corresponding to Ru(acac)$_3$ was eluted by $CH_2Cl_2-CH_3CN$ (20:1), followed by a blue compound corresponding to [**5**]ClO_4, which was eluted with $CH_2Cl_2-CH_3CN$ (20:3). Evaporation of the solvent mixture yielded the pure [**5**]ClO_4. Yield: 58 mg (46%). Anal. Calcd (found) for [**5**]ClO_4 ($Ru_2C_{35}H_{35}N_7O_{10}Cl$): C, 44.12 (44.27); H, 3.71 (3.65); N, 10.30 (10.48). Molar conductivity [Λ_M (Ω^{-1} cm^2 M^{-1})] in acetonitrile at 298 K: 126. IR [$\nu(ClO_4^-)$/cm^{-1}]: 1107, 629.

Synthesis of [6]ClO_4. The dinuclear complex [**5**]ClO_4 (50 mg, 0.052 mmol) and excess *m*-chloroperbenzoic acid (18 mg, 0.11 mmol) were dissolved in 20 mL of dichloromethane, and the mixture was stirred for 4 h under a N_2 atmosphere. The initial blue color of the solution gradually changed to violet. The solvent was removed under reduced pressure, and the residue was purified using a neutral alumina column. A purple-red compound corresponding to [**6**]ClO_4 was eluted by $CH_2Cl_2-CH_3CN$ (5:1). Evaporation of the solvent mixture yielded the pure compound [**6**]ClO_4. Yield: 16 mg (31%). Anal. Calcd (found) for [**6**]ClO_4 ($Ru_2C_{35}H_{35}N_7O_{12}Cl$): C, 42.68 (42.82); H, 3.58 (3.50); N, 9.96 (9.75). Molar conductivity [Λ_M (Ω^{-1} cm^2 M^{-1})] in acetonitrile at 298 K: 140. IR [$\nu(ClO_4^-)$/cm^{-1}]: 1107, 629.

Synthesis of [7]ClO_4. The dinuclear complex [**5**]ClO_4 (50 mg, 0.052 mmol) was dissolved in 20 mL of ethanol and refluxed for 16 h under a N_2 atmosphere. The initial blue color of the solution gradually changed to bluish-green. The solvent was removed under reduced pressure, and the residue was purified using a neutral alumina column. A green compound corresponding to [**7**]ClO_4 was eluted by $CH_2Cl_2-CH_3CN$ (4:1). Evaporation of the solvent mixture yielded the pure compound [**7**]ClO_4. Yield: 24 mg (46%). Anal. Calcd (found) for [**7**]ClO_4 ($Ru_2C_{37}H_{41}N_7O_{11}Cl$): C, 44.49 (44.62); H, 4.14 (4.28); N, 9.82 (9.73). Molar conductivity [Λ_M (Ω^{-1} cm^2 M^{-1})] in acetonitrile at 298 K: 117. IR [$\nu(ClO_4^-)$/cm^{-1}]: 1128, 630.

Synthesis of [8]ClO_4. The dinuclear complex [**5**]ClO_4 (50 mg, 0.052 mmol) and pyrazine (4.2 mg, 0.052 mmol) were dissolved in 20 mL of ethanol, and the mixture was heated to reflux for 8 h under a N_2 atmosphere. The initial blue color of the solution gradually changed to greenish-blue. The solvent was removed under reduced pressure, and the residue was purified using a neutral alumina column. A bluish-green compound corresponding to [**8**]ClO_4 was eluted by $CH_2Cl_2-CH_3CN$ (3:1). Evaporation of the solvent mixture yielded the pure compound [**8**]ClO_4. Yield: 16 mg (31%). Anal. Calcd (found) for [**8**]ClO_4 ($Ru_2C_{37}H_{36}N_8O_{10}Cl$): C, 44.80 (44.39); H, 3.66 (3.85); N, 11.30 (11.50). Molar conductivity [Λ_M (Ω^{-1} cm^2 M^{-1})] in acetonitrile at 298 K: 112. IR [$\nu(ClO_4^-)$/cm^{-1}]: 1107, 634.

Crystal Structure Determination. Single crystals of [**1**]ClO_4, [**2**]ClO_4, and [**3**]ClO_4 were grown by slow evaporation of a 1:1 dichloromethane−hexane solution. The crystals of [**1**]ClO_4, [**2**]ClO_4, and [**3**]ClO_4 contain $2H_2O$ as the solvent of crystallization. X-ray data of [**1**]ClO_4/[**3**]ClO_4 and [**2**]ClO_4 were collected using Enraf-Nonius CAD-4 (MACH-3) and Bruker SMART APEX CCD single-crystal X-ray diffractometers, respectively. The structures of [**1**]ClO_4/[**3**]ClO_4 and [**2**]ClO_4 were solved and refined by full-matrix least-squares techniques on F^2 using the *SHELX-97* and *SHELX-97* (*SHELXTL* program package), respectively.[21] The absorption corrections for [**1**]ClO_4/[**3**]ClO_4 and [**2**]ClO_4 were done by ψ scan and SADABS, respectively, and all of the data were corrected for Lorentz and polarization effects. H atoms were included in the refinement process as per the riding model.

The $-CH_2-CH_3$ group of [**2**]ClO_4 is disordered, with C26 and C27 atoms having two different positions with equal occupancy and having large thermal vibrations; the corresponding constraints have been used during refinement, and H atoms for C26 and C27 are not fixed.

Acknowledgment. Financial support received from the Department of Science and Technology and Council of Scientific and Industrial Research, New Delhi, India, is gratefully acknowledged. X-ray structural studies for [**1**]ClO_4 and [**3**]ClO_4 were carried out at the National Single Crystal Diffractometer Facility, Indian Institute of Technology—Bombay. Special acknowledgment is made to the Sophisticated Analytical Instrument Facility (SAIF), Indian Institute of Technology—Bombay, for providing the NMR and EPR facilities.

Supporting Information Available: X-ray crystallographic data in CIF format, electrospray mass spectra of [**1**]ClO_4−[**4**]ClO_4 in CH_3CN (Figure S1), H bonding in [**1**]ClO_4·$2H_2O$ (Figure S2), and H-bonding parameters in [**1**]ClO_4·$2H_2O$ (Table S1). This material is available free of charge via the Internet at http://pubs.acs.org.

IC0514288

(21) Sheldrick, G. M. *SHELX-97, program for crystal structure solution and refinement*; University of Göttingen: Göttingen, Germany, 1997.